IOPscience iopscience.iop.org

Home Search Collections Journals About Contact us My IOPscience

Optical absorption spectra associated with an impurity in a corner

This article has been downloaded from IOPscience. Please scroll down to see the full text article.

1995 J. Phys.: Condens. Matter 7 6493

(http://iopscience.iop.org/0953-8984/7/32/015)

View the table of contents for this issue, or go to the journal homepage for more

Download details:
IP Address: 171.66.16.151
The article was downloaded on 12/05/2010 at 21:55

Please note that terms and conditions apply.

J. Phys.: Condens. Matter 7 (1995) 6493–6500. Printed in the UK

Optical absorption spectra associated with an impurity in a corner

Zhen-Yan Deng†‡, Hong Zhang‡, Jian-Lin Shi‡ and Jing-Kun Guo‡

† China Centre of Advanced Science and Technology (World Laboratory), PO Box 8730, Beijing 100080, People's Republic of China

‡ The State Key Laboratory of High Performance Ceramics and Superfine Microstructure, Shanghai Institute of Ceramics, Chinese Academy of Sciences, Shanghai 200050, People's Republic of China

Received 16 January 1995, in final form 1 May 1995

Abstract. We calculate the optical absorption spectra associated with an impurity in a corner of well material surrounded by barrier material. The results show that there are new peaks and a large extension for the optical transitions in the corner compared with those in the bulk. The dependence of the optical absorption spectra on the dielectric mismatch between the well material and the barrier material is also discussed.

1. Introduction

Low-dimensional structures having quantum confinement in one, two or all three dimensions (quantum wells, quantum well wires and quantum dots) have attracted both theoretical and experimental attention in the past few years, due to their potential applications in microelectronics and optical modulation technology. The presence of impurities in these structures contributes to additional responses when external probes are applied to these systems. The variational approach is an effective method for the study of impurity states in low-dimensional systems. The impurity binding energies obtained by the variational theory have been successfully compared with a variety of experimental results by many researchers [1–5]. Usually, the step structures exist at the interfaces of low-dimensional structures [6], which affect their electronic and optical properties considerably. When the sizes of the step structures are large enough, we can model them as the corners [6]. In fact, corner structures exist in any sample, such as a semiconductor corner surrounded by the vacuum. The corner model can also be used in the V-shaped grooves in the surfaces [7].

In our previous paper [6], we have studied the electronic and shallow impurity states in the corners of two orthogonal surfaces using the variational approach. The results showed that the impurity binding energy in the corners approaches that of the third impurity excited states in the bulk. In this paper, we study the optical transitions from the first valence miniband to donors in the same corner structures further. In section 2, we calculate the density of impurity states in the corners. In section 3, we calculate the optical transition probability. The numerical results and discussion are presented in section 4.

0953-8984/95/326493+08$19.50 © 1995 IOP Publishing Ltd

2. Density of impurity states

In the effective-mass approximation, the electronic Hamiltonians excluding and including an impurity in the corner can be written

$$H^{(0)}(r) = \frac{|P|^2}{2m} + V_e(r) + V(r) \tag{1}$$

and

$$H(r) = \frac{|P|^2}{2m} + V_{ion}(r) + V_e(r) + V(r) \tag{2}$$

where $\boldsymbol{P}$ and r are the electron momentum and coördinate, respectively, and m is the electron-band effective mass; $V_e(r)$ is the electron image potential and $V_{ion}(r)$ is the sum of impurity ion and its image potentials inside the corner [6]. The electron-confining potential well is given by

$$V(r) = \begin{cases} 0 & x > 0, y > 0 \\ \infty & \text{elsewhere.} \end{cases} \tag{3}$$

The trial wavefunctions and energy levels for ground electronic states are [6]

$$\phi^{(1)}(r) = N_0 \begin{cases} \sin(k_x x)\sin(k_y y) & \epsilon \geqslant 1 \\ xy\exp[-(x+y)/\alpha] & \epsilon < 1 \end{cases} \tag{4}$$

and

$$E_1 = \begin{cases} 0 & \epsilon \geqslant 1 \\ \min\limits_{\alpha}\langle\phi^{(1)}(r)|H^{(0)}(r)|\phi^{(1)}(r)\rangle & \epsilon < 1 \end{cases} \tag{5}$$

where N_0 is the normalization constant, k_x, $k_y \to 0$ and α is the variational parameter; $\epsilon = \epsilon_1/\epsilon_2$ is the ratio of the dielectric constant ϵ_1 inside to the dielectric constant ϵ_2 outside the corner.

The trial wavefunction for the ground impurity state that we take is written [6]

$$\psi(r) = N\frac{xy}{x^2+y^2+\beta^2}\exp\left(\frac{-[(x-x_0)^2+(y-y_0)^2+z^2]^{1/2}}{\lambda}\right) \tag{6}$$

where N is the normalization constant, and β and λ are the variational parameters; $r_0 = (x_0, y_0, 0)$ is the position of the impurity inside the corner. The impurity binding energy in the corner is obtained as follows:

$$E_b = E_1 - \min_{\beta,\lambda}\langle\psi(r)|H(r)|\psi(r)\rangle. \tag{7}$$

Assuming that the corner is not too small, we could treat the impurity position as a continuous random variable. Provided that the impurities exist only inside the corner and there is no intentional doping, the density of impurity states per unit binding energy can be defined as

$$g(E_b) = \frac{1}{S}\int_{L(E_b)}\frac{\mathrm{d}l}{|\nabla_{r_0}E_b(r_0)|} \tag{8}$$

where S is the area of the corner, $L(E_b)$ is the portion of the line $E_b = E$ lying within the corner and ∇_{r_0} means the gradient with respect to the impurity position. The density of impurity states is then obtained by a histogram method [8] for a mesh of points uniformly distributed in the corner. The number of points used in the mesh is increased systematically until fluctuations in the density of states are smoothed out.

3. Optical absorption spectra

For optical transitions from the first valence miniband to a donor level, we have for the initial state

$$|i\rangle = \phi^{(1)}(\boldsymbol{r})u_i(\boldsymbol{r})\exp(\mathrm{i}k_z z) \tag{9}$$

and for the final state

$$|f\rangle = \psi(\boldsymbol{r})u_f(\boldsymbol{r}) \tag{10}$$

where $u_i(\boldsymbol{r})$ and $u_f(\boldsymbol{r})$ are the periodic parts of the Bloch state for the initial and final states, respectively.

Taking the energy origin at the bottom of the first conduction miniband, we have for the energy of the initial state

$$E_i = -\epsilon_g - \frac{\hbar^2 k_z^2}{2m_v} \tag{11}$$

where m_v is the effective mass of the valence band and ϵ_g is given by

$$\epsilon_g = E_g + E_1^c + E_1^v \tag{12}$$

with E_g being the bulk band gap of well material and E_1^c (E_1^v) being the ground-state energy of the first conduction (valence) miniband. The energy of the final state is

$$E_f = -E_b(\boldsymbol{r}_0) \tag{13}$$

where $E_b(\boldsymbol{r}_0)$ is the binding energy of the donor impurity.

The transition probability per unit time for transitions from the first valence miniband to donor impurity associated with the impurity located at the position $\boldsymbol{r}_0$ is proportional to the square of the matrix element of the electron–photon interaction H_{int} between the wavefunctions of the initial state (valence) and final (impurity) state [9–13]:

$$W(\omega, \boldsymbol{r}_0) = \frac{2\pi}{\hbar}\sum_i |\langle f|H_{int}|i\rangle|^2 \delta(E_f - E_i - \hbar\omega) \tag{14}$$

with $H_{int} = C\boldsymbol{e}\cdot\boldsymbol{p}$, where $\boldsymbol{e}$ is the polarization vector in the direction of the electric field of the radiation, $\boldsymbol{p}$ is the momentum operator and C is a pre-factor that describes the effects of the photon vector potential [14]. Following the effective-mass approximation, the above matrix element may be written [9–13]

$$\langle f|H_{int}|i\rangle \simeq C\boldsymbol{e}\cdot\boldsymbol{P}_{fi}S_{fi} \tag{15}$$

with

$$\boldsymbol{P}_{fi} = \frac{1}{\Omega}\int_\Omega u_f^*(\boldsymbol{r})\boldsymbol{p}u_i(\boldsymbol{r})\,\mathrm{d}\boldsymbol{r} \tag{16}$$

and

$$S_{fi} = \int F_f^*(\boldsymbol{r})F_i(\boldsymbol{r})\,\mathrm{d}\boldsymbol{r} \tag{17}$$

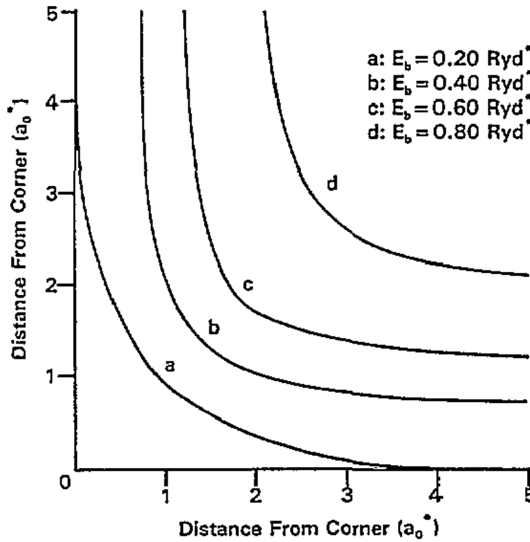

Figure 1. The contours of the impurity binding energy in the corner, where the dielectric constant ratio $\epsilon = 1$.

where Ω is the volume of the unit cell and $F_f(r)$ ($F_i(r)$) is the envelope function for the final (initial) state. Then equation (14) can be simplified further:

$$W(\omega, r_0) = \frac{L_0}{\hbar^2} \left(\frac{m_v}{2}\right)^{1/2} |C|^2 |\mathbf{e} \cdot P_{fi}|^2 |S_{fi}(r_0, k_z(\Delta))|^2 \frac{Y(\Delta)}{\Delta^{1/2}} \tag{18}$$

where L_0 is the length in the z direction and $Y(\Delta)$ is the step function with

$$\Delta = \hbar\omega + E_b(r_0) - \epsilon_g. \tag{19}$$

The total transition probability per unit time is given by

$$W(\omega) = \frac{1}{S} \int_S W(\omega, r_0)\, \mathrm{d}r_0. \tag{20}$$

The above integrals were calculated numerically.

4. Results and discussion

Figure 1 shows the contours of the impurity binding energy in the corner, where the ratio ϵ of the dielectric constant inside to that outside the corner equals unity. In figure 1, the energy is in units of effective Rydbergs Ryd* $= m_c e^4/2\hbar^2\epsilon_1^2$ and the length is normalized to the effective Bohr radius $a_0^* = \hbar^2\epsilon_1/m_c e^2$, with m_c the effective mass of the conduction band. In our practical calculation, the following parameters are used: $m_c = 0.067m_0$, $m_v = 0.30m_0$ and $\epsilon_1 = 13.1\epsilon_0$ for GaAs, and $\epsilon_2 = 10.1\epsilon_0$ for AlAs [6,9], where m_0 and ϵ_0 are the free-electron mass and the vacuum static dielectric constant, respectively; $m_c = 0.11m_0$, $m_v = 0.45m_0$ and $\epsilon_1 = 9.29\epsilon_0$ for CdSe, and $\epsilon_2 = 10.1\epsilon_0$ for ZnTe [15]; for the general case, we set $m_v = 5.0m_c$. Here, we assumed an averaged parabolic valence hole band with the mixing of the light- and heavy-hole bands neglected [9]. In addition, the integral region that we adopted in the corner is $S = 10a_0^* \times 10a_0^*$.

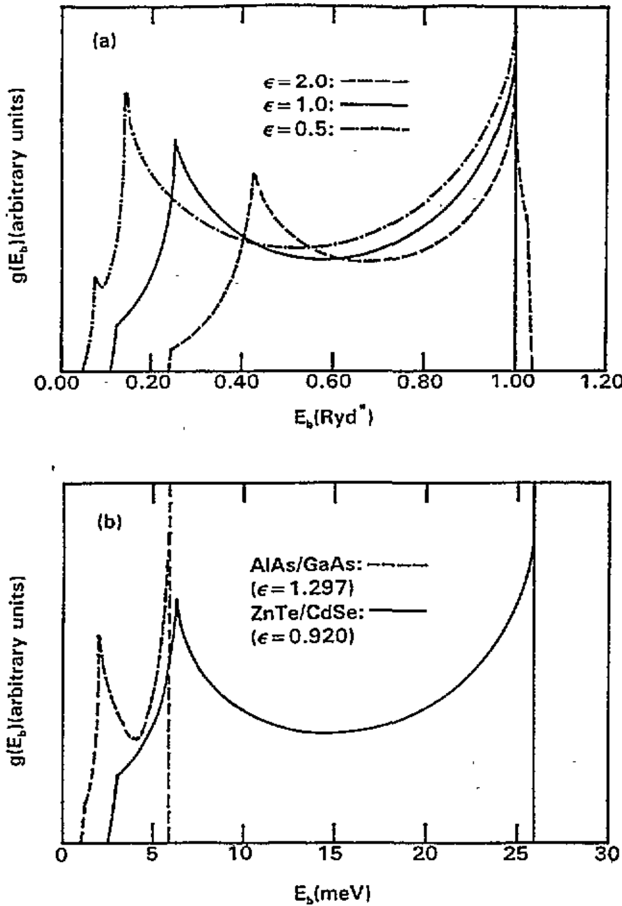

Figure 2. The densities of impurity states (a) in the corner with three different dielectric mismatches and (b) in the AlAs–GaAs and ZnTe–CdSe corners.

Figure 2 shows the densities of impurity states in the corners with different dielectric mismatches. In figure 2, it is apparent that new peaks appear in the density of impurity states in the corner compared with those in the bulk, and the density of impurity states extends towards the low-binding-energy region considerably. From figure 2(a), we can see that, the smaller the dielectric constant ratio ϵ, the larger is the extension in the density of impurity states in the corner (in units of effective rydbergs). When the ratio $\epsilon = 2$, the density of impurity states extends slightly to the high-binding-energy region. The widths of the extension in the density of impurity states in the corner are 0.80 Ryd*, 0.89 Ryd* and 0.94 Ryd* for the ratios $\epsilon = 2.0$, 1.0 and 0.5, respectively. From figure 2(b), we can also see that the extension in density of impurity states in the ZnTe–CdSe corner (23.45 meV) is much larger than that in AlAs–GaAs corner (4.70 meV).

Figure 3 shows the possible optical transitions from the first valence miniband to donor band, where $\hbar\omega_1$ and $\hbar\omega_2$ represent the transition energies from the top edge of the first valence miniband to the bottom edge and the top edge, respectively, of the donor band. The optical absorption spectra associated with donors in the corners with different dielectric mismatches are shown in figure 4, where $E_j = \hbar\omega_j - E_g$ $(j = 1, 2)$.

Features in the density of impurity states in figure 2, new peaks and a large extension

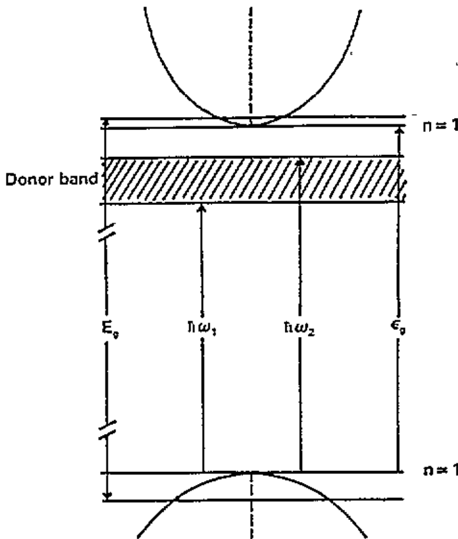

Figure 3. Schematic representation of some possible optical transitions from the first valence miniband to the donor band in the corner, where the parabolae represent the energy dispersions of the first conduction and valence minibands in the z direction.

also appear in the optical absorption spectra in the corner compared with those in the bulk. Also, the smaller the dielectric constant ratio ϵ, the larger the extension in optical absorption spectra in the corner (in units of effective rydbergs), as shown in figure 4(a), and the extension in optical absorption spectra in the ZnTe–CdSe corner is much larger than that in AlAs–GaAs corner, as shown in figure 4(b).

The above results are interesting and their physical interpretation is as follows. Because of the confinement of electrons in the corner, the electronic wavefunctions near the corner for impurity states are very similar to that of the $3d_{xy}$ impurity excited state in the bulk [6] and the impurity binding energy in the corner tends to the value $\frac{1}{9}$ Ryd* of the third impurity excited states in the bulk. This is the reason why the density of impurity states in the corner extends largely towards the low-binding-energy region. When the dielectric constant ratio changes from $\epsilon > 1$ to $\epsilon < 1$, the impurity ion image potentials change from negative to positive, and the impurity binding energy decreases with decrease in the dielectric constant ratio [6]; so the extension in the density of impurity states in the corner is large when the ratio ϵ is small. The wider extension in the density of impurity states in the ZnTe–CdSe corner than in the AlAs–GaAs corner is due to the heavier conduction effective mass and smaller dielectric constant in CdSe than in GaAs. In figure 3, we can see that the width for optical transitions from the first valence miniband to the donor level is related closely to the width of the donor band. In a sense, the width of the donor band is a representation of the width of the optical absorption spectra; so the extension appearing in the density of impurity states in the corner, in a similar way, occurs in its optical absorption spectra. In addition, the new peaks in the density of impurity states and optical absorption spectra are related to the important impurity positions in the corner. The first and second peaks on the low-energy sides of the density of impurity states or on the high-energy sides of the optical absorption spectra corresponds to the impurity positions near the corner and the positions far from the corner but near one side of it, respectively. The peaks on the high-energy sides of the density of impurity states and the absorption edges correspond to the impurity positions in the bulk.

Summing up, we have studied the density of impurity states and the optical absorption spectra associated with the impurity in the corners. The results indicate that new peaks and a large extension appear for the optical transitions from the first valence miniband to the

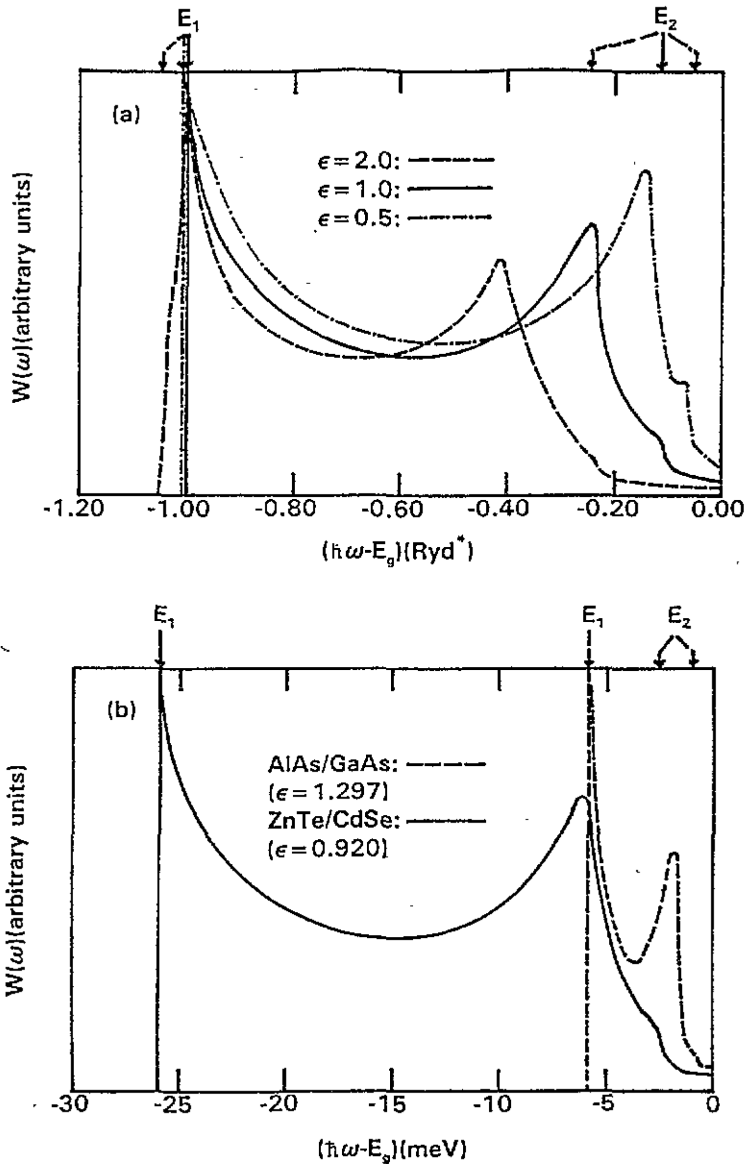

Figure 4. Optical absorption probability per unit time for the transitions from the first valence miniband to donor band (a) in the corner with three different dielectric mismatches and (b) in the AlAs–GaAs and ZnTe–CdSe corners.

donor band in the corners, compared with those in the bulk. The results also indicate that the extensions in the density of impurity states and optical absorption spectra in the corner are large when the dielectric constant ratio ϵ is small. Our corner model can be used only for the interface step structures with large sizes and for the practical corner of well material surrounded by the barrier material, but not for the interface structures with monolayer steps. In any sample there are corners of semiconductor well material surrounded by vacuum, and in many samples corners surrounded by barrier material can also be found. We hope that our theoretical results stimulate further experimental investigations.

Acknowledgments

One of the authors (Jian-Lin Shi) would like to thank the National Natural Science Foundation for support under grant 59452001 and the Young Scientist Foundation of Chinese Academy of Sciences.

References

[1] Oliveira L E and Falicov L M 1986 *Phys. Rev.* B **34** 8687
[2] Fraizzoli S, Bassani F and Buczko R 1990 *Phys. Rev.* B **41** 5096
[3] Barmby P W, Dunn J L and Bates C A 1994 *J. Phys.: Condens. Matter* **6** 751
[4] Carneiro G N, Weber G and Oliveira L E 1995 *Semicond. Sci. Technol.* **10** 41
[5] Latgé A, Porras-Montenegro N and Oliveira L E 1995 *Phys. Rev.* B **51** 2259
[6] Deng Z Y, Zhang H and Guo J K 1994 *J. Phys.: Condens. Matter* **6** 9729 and references therein
[7] Vacek K, Sawada A and Usagawa T 1994 *Appl. Phys. Lett.* **65** 3096
[8] Weber G, Schulz P A and Oliveira L E 1988 *Phys. Rev.* B **38** 2179
[9] Oliveira L E and Perez-Alvarez R 1989 *Phys. Rev.* B **40** 10460
[10] Porras-Montenegro N and Oliveira L E 1990 *Solid State Commun.* **76** 275
[11] Weber G and Oliveira L E 1990 *Mater. Sci. Forum* **65–6** 135
[12] Latgé A, Porras-Montenegro N and Oliveira L E 1992 *Phys. Rev.* B **45** 6742
[13] Deng Z Y and Guo J K 1995 *J. Phys.: Condens. Matter* **7** 1327
[14] Bassani F and Parravicini G P 1975 *Electronic States and Optical Transitions in Solids* ed R A Ballinger (Oxford: Pergamon)
[15] Madelung O 1982 *Landolt–Börnstein New Series, Zahlenwerte und Funktionen aus Naturwissenschatten und Technik Neue Serie* Group III, vol 17 (Berlin: Springer)